

Surface Treatment of Polylactic Acid Fiber by Starch Nanocrystals and Interface Modification of Polylactic Acid Fiber-Reinforced Starch Composites

Ming Sun¹, Huihuang Ma¹, Shaoxia Yang¹, Yingxuan Chen¹, Haiyan Liu¹ and Xiaodong Zhou^{1,*}

¹State Key Laboratory of Chemical Engineering, East China University of Science and Technology, Shanghai 200237, China

Abstract: The surface of polylactic acid fiber (PLAF) was treated with self-manufactured starch nanocrystals (SNCs) to improve its interfacial adhesion with the starch matrix. Determination of optimum dispersion conditions of SNCs dispersion by transmittance. The effects of direct oscillatory deposition, chemical grafting SNCs modification, and SNCs dispersion concentration on the surface treatment effect of PLAF and its interfacial bonding with starch matrix were investigated. The results showed that the SNCs were successfully introduced into the PLAF surface, moreover, the modifying effect of the chemical grafted SNCs was better than the direct oscillatory deposition, the distribution of SNCs particles was more uniform on the fiber surface, strong chemical bonding to the fiber surface, make up for the surface damage of the fibers caused by aminolysis. At the SNCs dispersion concentration of 10 g/L, the PLAF tensile strength could be maintained at 582 MPa, a large amount of starch was evenly attached to the surface after pulling out. It showed that a strong interface bond with the starch matrix, the highest IFSS value was 2.57 MPa and the increase was by about 63 %. Therefore, the introduction of SNCs for interfacial modification of PLAF is of great significance and deserves further exploration.

Keywords: Polylactic acid fiber, Starch nanocrystals, Surface treatment, Interface, Strength.

INTRODUCTION

With the continued development of the social economy, plastic products were widely utilized in human production and life. However, the lack of oil resources and the harm of traditional plastic waste have brought great challenges to the development of human society, and sustainable new biodegradable materials have emerged at the historic moment [1, 2]. The biodegradability and environmental friendliness of natural polymers have attracted wide attention from academia and industry. Some degradable biomass such as starch, cellulose, protein, and biopolymers produced by natural resources or microorganisms have also become the objects of research and use. Starch raw materials are easy to obtain, cheap, and widely used, and are considered as one of the most promising biodegradable materials with development potential [3, 4]. However, the poor mechanical properties of the starch material itself limit its development and application to some extent [5-7].

It was found that the mechanical properties of the starch composites could be improved by introducing fibers into the starch material as enhancers [8]. Among

them, PLAF has good mechanical properties, biocompatibility, and breakdown [9]. However, the interaction and affinity with starch are poor, and it was difficult to form an effective interface bond in the recombination process of PLAF and starch [10]. It was necessary to surface treat polylactic fibers [11] To improve its interface compatibility with starch, thus improving the mechanical properties of composite materials, and widening its field of application.

Starch nanocrystals (SNCs) have special multi-scale effects, good mechanical properties, and high surface energy, and have a similar chemical structure to starch, which was a synthetic nano-enhancer material [12]. It could be introduced to the surface of the polylactic fiber to improve its interface compatibility with the starch matrix. Moreover, polylactic acid fibers and starch were completely degradable materials, which were of great importance for the practice of developing green protection and the environment.

In this paper, we introduced SNCs to investigate the effects of direct oscillatory deposition and chemical grafting modification, the dispersion concentration of different SNCs on PLAF surface treatment, and the interfacial bond performance to the starch matrix. The chemical properties of the modified PLAF surface were characterized by infrared spectroscopy, and the surface morphology of the modified PLAF was observed by scanning electron microscopy. The

*Address correspondence to this author at the State Key Laboratory of Chemical Engineering, East China University of Science and Technology, No. 130, Meilong Road, Xuhui District, Shanghai 200237, China; Tel: +86 21 64253757; E-mail: xdzhouecust@126.com

mechanical properties of PLAF and the interfacial properties of PLAF-reinforced starch matrix were studied through tensile test and pull-out test, to further improve the properties of PLAF-starch composites.

2. EXPERIMENTAL

2.1. Materials

Waxy maize starch was purchased from Shanghai Xian Ding Biotechnology Co, Ltd. Corn starch was purchased from Huanglong Food Industry Co., Ltd. polylactic acid fiber was purchased from Shenzhen Guanghua Weiye Industrial Co., Ltd. Glycerin was provided by Shanghai Maclin Biochemical Technology Co., Ltd. Hexanediamine, glutaraldehyde, and isopropanol were provided by Shanghai Ling Feng Chemical Reagent Co., Ltd. Glycerol was provided by Shanghai Macklin Biochemical Co., Ltd. Concentrated sulfuric acid was provided by Sinopharm Chemical Reagent Co., Ltd. Anhydrous ethanol was provided by Shanghai Titan Technology Co., Ltd.

2.2. Pretreatment of PLAF

Some untreated PLAF was immersed in 40 of the aqueous ethanol solutions for 3 h to remove oily impurities from the fiber surface and removed for drying. Spread the processed PLAF evenly and save for standby [13].

2.3. Preparation of the Dispersion Solution of SNCs

Preparation of SNCs by acid hydrolysis method [14], called 36.725 g of waxy corn starch and 250 mL sulfuric acid solution (3.16 mol/L) and stirred continuously in a 40°C heated water bath for 5 days. Then it was centrifuged with deionized water to neutralize, and under lyophilized vacuum, weighed and ground. The appropriate amount of SNCs was taken in ethanol aqueous solution and sonicated in an ice-water bath to obtain SNCs dispersion.

2.4. Surface Modification of PLAF

1. Direct oscillatory deposition of SNCs to the PLAF surface

The pretreated PLAF was immersed in starch nanocrystals suspension and it was continuously oscillated in a 40°C thermostatic oscillator for 1h, dried, washed, and then dried, yielding PLAF of directly oscillating deposited SNCs, namely PLAF-SCNs.

2. Chemically modified grafted SNCs to the PLAF surface

Pre-treated PLAF was placed in the adipose/isopropanol domain solution (0.04 g/mL) for 20 minutes, followed by isopropanol, deionized water wash, and drying. Reaction in glutaraldehyde solution (2.0 % by weight) for 1 h, rinsed and dried with deionized water. Finally, the aldehydes PLAF was placed in different contents of SNCs dispersion (5, 10, 15, 20, 25 g/L), with a constant temperature oscillation reaction at 40°C for 6 h, washed, dried, and stored for reserve, to obtain PLAF of different concentrations of SNCs, *i.e.* PLAF-g-SCNn.

2.5. Preparation of Fiber Extraction Samples

Corn starch emulsion was first stirred at constant temperature for 0.5 h, pregelatinized before adding glycerol and then stirred at constant temperature for 3 h. After the reaction, the ultrasonic deg was poured into the self-made mold fixed with PLAF. The fiber was removed for 10 mm, dried at room temperature for 12 h, and then baked at a constant temperature at 40 for 12 h. After cutting, put into the constant wet dryer for reserve [15].

3. TESTING AND CHARACTERIZATION

3.1. Infrared Spectroscopic Analysis (FTIR)

A type Thermo Nicolet 6700 infrared spectrometer was used to characterize the functional mass changes of waxy maize starch and SNCs powder, and ATR to test the changes before and after grafted SNCs was measured in the wave number range of 400-4000 cm^{-1} .

3.2. Scanning Electron Microscopy (SEM)

Characterization analysis was performed using a JSM-6360LV type scanning electron microscope, scattering waxy corn starch and SNCs powder onto a sample table with adhesive conductive adhesive to observe their surface micromorphology. The microscopic surface morphology of the PLAF before and after the grafting SNCs was also observed, the grafting density was observed, and the fiber surface adhesion resin after pulling out the experiment. Samples were glued to the sample table with a vacuum platinum spray time of 30 s, test acceleration voltage of 15 kv, and EM resolution of 3.0 nm.

3.3. Analysis of the Laser Granularity Distribution

A type ZEN3600 laser granular meter was used to determine the particle size of the SNCs. At the time of testing for the same sample, 3-5 concentrations of

different SNCs should be selected for the test, and the concentration change does not affect the size of the particle size as the appropriate concentration. At this appropriate concentration, the particle diameter of the sample was measured with deionized water as the medium. About 1mL, one sample was repeated three times. If there was poor reproducibility, unsatisfactory results should be removed or samples could be taken.

3.4. Thermal Stability Analysis (TG)

Type STA449F3 high temperature synchronous thermal analyzer was used to determine the thermal stability of the sample, weighing approximately 5 mg of wax corn starch and SNCs powder and put into the crucible. The test conditions were: nitrogen atmosphere, room temperature rises to 600°C, heating speed of 10°C/min, and nitrogen purge flow rate of 30 mL/min.

3.5. Optical Transmittance Analysis (UV)

The transmittance of SNCs suspension at 600 nm was determined using a TU-1810 type UV visible spectrophotometer using pure dispersion medium as a blank control.

3.6. Calculation of the Moisture Absorption Rate

PLAF was cut into very small sections, and thin fibers of different treatments were pressed on an FW-4/A press with a pressure of 20 MPa. The fibers after the pressing were placed in a 70°C oven for 12 h, weighing the mass, and then in a constant temperature and humidity tank of 90 % humidity for 72 h, and again weighing the mass. Fibers were tested 3 times for each treatment method. The moisture absorption rate of PLAF could be calculated from the following equation (1)

$$W = \frac{m_t - m_o}{m_o} \times 100\% \quad (1)$$

Where W is the moisture absorption rate of PLAF, m_o and m_t represent the mass of the fibers before and after moisture absorption, respectively.

3.7. Fiber Tensile Strength Test

The tensile strength of polylactic fiber single filaments was measured using an optical microscope and type YG004A electron single fiber power instrument. Its working principle is shown in Figure 1. The diameter measurement of the fiber single filament

is as follows: first, use double-sided glue to fix the treated PLAF single filaments on a clean and dry glass sheet, and then measure the diameter of the fiber single filament at three different positions using an optical microscope. Therefore, the results were the diameter of the fiber single filament, and the cross-sectional area of the fiber could be calculated through the diameter. Polylactic single filaments were stretched using a single filament power instrument with a clamp length of 10mm and a tensile speed of 1 mm/min. Due to the high dispersion of single filament tensile strength, the two-parameter Weibull model was used to process the data. At least 30 effective samples were measured for polylactic fibers under different treatment conditions. The tensile strength could be calculated by Equations (2).

$$\sigma = \frac{4F}{\pi d^2} \quad (2)$$

Where σ is the tensile strength of the fiber filament, F is the current fiber filament fracture strength, and d is the fiber filament diameter.

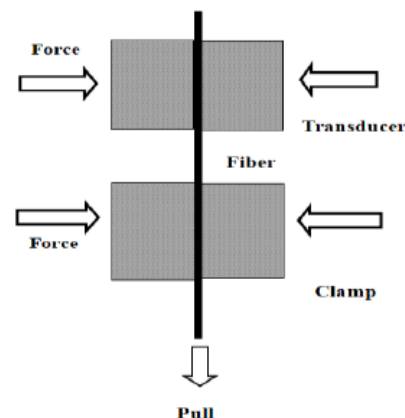


Figure 1: Schematic illustration of the fiber tensile strength test.

3.8. Fiber Interface Shear Strength Test

An optical microscope and UH2502 universal testing machine were used to conduct fiber pull-out experiments to explore the interfacial bonding properties of PLAF. Its working principle is shown in Figure 2. The fiber diameter was measured in the same as the tensile strength test. The test speed was 1mm/min and at least 30 valid samples were measured for PLAF under different treatment conditions. Assuming that the shear stress at the fiber interface is evenly distributed along the embedding length in the matrix, the interface shear strength could be processed

analyzed according to the two-parametric Weibull model. According to the Kelly / Tyson formula [16] to calculate the interface shear strength:

$$\tau = \frac{F_{max}}{\pi dl} \quad (3)$$

Where F_{max} was the maximum load measured before removal from the matrix; d and l are respectively the diameters of the fiber and the integrated length. For the tests, the shear stress at the interface was assumed to be evenly distributed along the embedded length. The IFSS was also calculated based on a two-parameter Weibull model

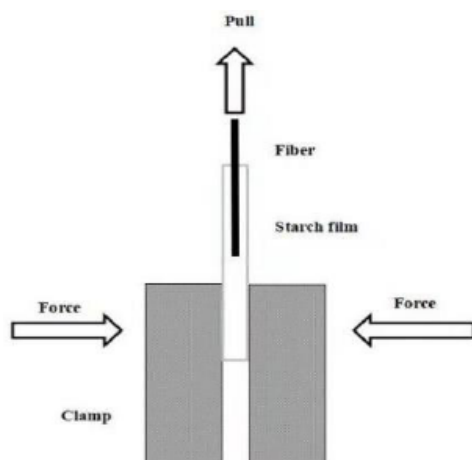


Figure 2: Schematic illustration of the fiber pull-out test.

4. RESULTS AND DISCUSSION

4.1. Analysis of the Dispersal Stability of the Starch Nanocrystals Suspension

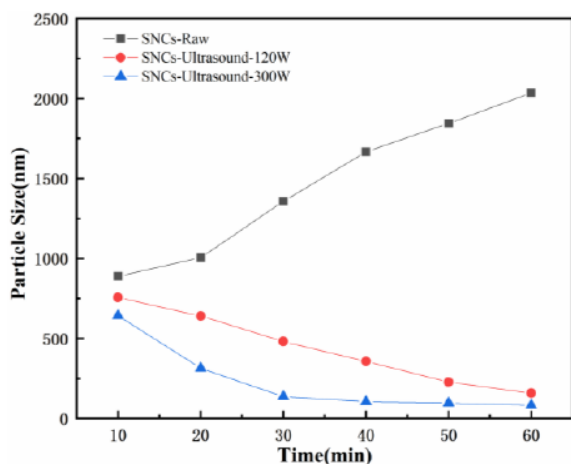


Figure 3: Effects of different power ultrasonic treatments on the particle size of SNCs.

As shown in Figure 3, SNCs dispersion without sonication stabilized on the nanoscale for a short

period, but particle size increased over time and met [17]. The behavior was serious, even reaching the micron level. However, in SNCs after ultrasound treatment, the reunion effect was weakened, in which 300 W ultrasound treatment was more obvious than 120 W ultrasound effect, and high-power ultrasound had a stronger instantaneous cavitation effect [18]. The reunited starch nanocrystals could be dispersed into smaller grades of nanoparticles in a short time, and the best effect was about 30 min, and the average particle size was about 150 nm. The continued ultrasound effect was not obvious. Therefore, ultrasound 30min was taken as the optimal ultrasound time in the subsequent experiments.

It could be seen from Figure 4(a) that the SNCs of 300 W high-power ultrasound remain uniformly dispersed after 1 h. Because the instantaneous cavitation of high-power ultrasound was stronger, the agglomeration effect was effectively avoided. As shown from Figure 4(b), when the PH was neutral or weakly alkaline, the resting SNCs dispersion was not significantly stratified, and the dispersion was better stable. Because the lower the PH of the solution, the lower the potential of the dispersion, the repulsion between the nanoparticles was insufficient to overcome the effects of hydrogen bonding forces and gravity. We could see from Figure 4(c) that the high dispersion of SNCs has less light transmittance in a short time, but the higher the particles, the more likely it was to reunite, and only the SNCs of small particles remain in the upper clear liquid. Figure 4(d) showed that different dispersion media have a great impact on the dispersion stability of SNCs, where the dispersion stability of anhydrous ethanol was better than that of water and cyclohexane. Because the anhydrous ethanol polarity was moderate, the hydrogen bond pulls up the molecular chain of the SNCs, and it also helps to remove the impurities on the fiber surface and increase the specific surface area of the fiber in contact with the SNCs.

4.2. Surface Modification of PLAF

(1) The Principle of Grafting SNCs on PLAF Surface

The PLA fiber surface was aminated by hexamethylene diamine, carboxyl, and ester group in the polylactic acid break, form amide bond, and the aldehyde group, and a lot of hydroxyl group with the aldehyde group, and glutaraldehyde could make PLAF and SNCs crosslink, forming SNCs network structure, further improve the effectiveness of the chemical bond,

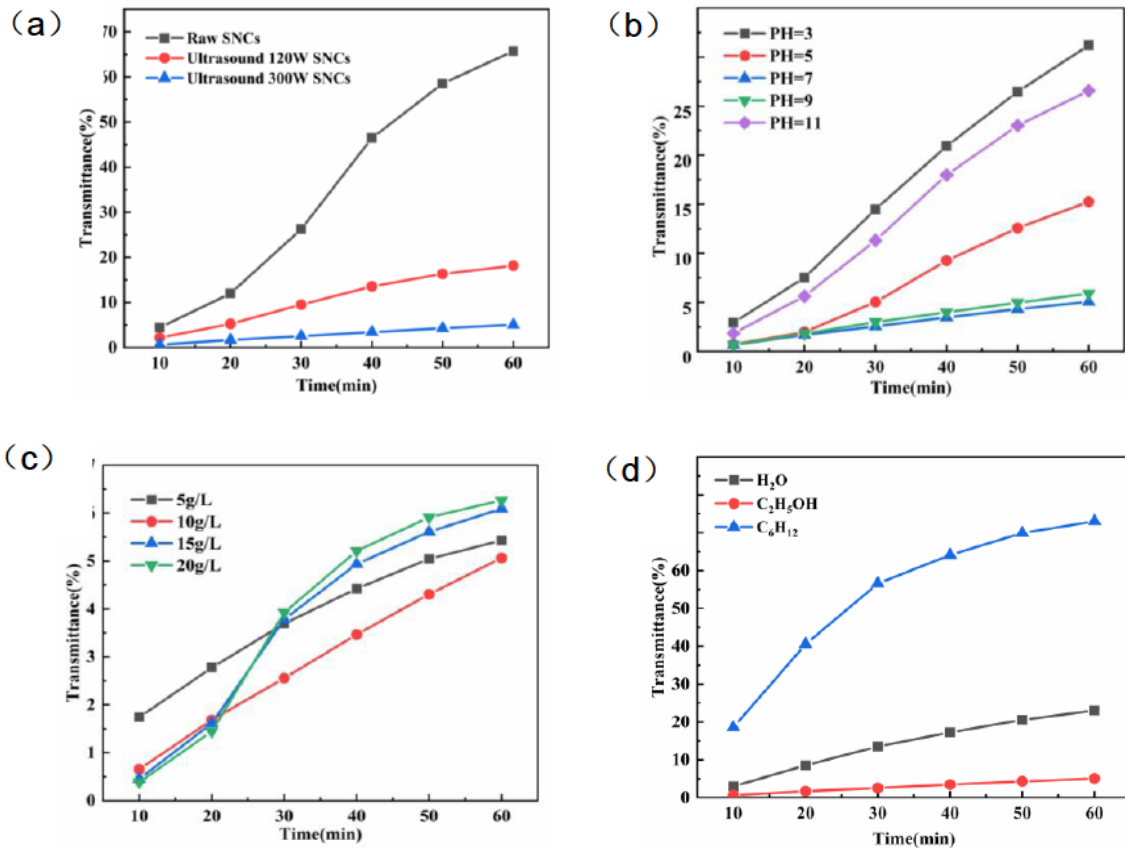


Figure 4: Effects of different treatment conditions on the transmittance of SNCs. (a) power ultrasonic treatments, (b) PH, (c) concentrations, (d) dispersed media.

improve the interface performance, the specific reaction process was shown in Figure 5:

(2) FTIR Analysis

It was shown from Figure 6 that the hydroxy peak of PLAF of directly oscillatory deposited SNCs was slightly convex and larger compared with unmodified PLAF, indicating that the binding effect of direct oscillatory deposited SNCs to PLAF was not good. However, PLAF modified by chemical grafting SNCs showed a broad peak at 3410 cm^{-1} , and here was the

extended vibration absorption peak of the O-H of the SNCs, at 2920 cm^{-1} . The absorption peak at the broadening was due to the effect of the enhanced C-H telescopic vibration absorption peak on the methylene group of the grafted SNCs at 1640 cm^{-1} . The vibration absorption peak of the hydrogen bonds within the starch molecule was indicated. In addition, the PLAF of the grafted SNCs was found at 1620 cm^{-1} , $1200\sim 1000\text{ cm}^{-1}$. The shape of the absorption peak at the position changes, mainly because the PLAF was affected by the elongating vibration absorption peak of the C-O-C

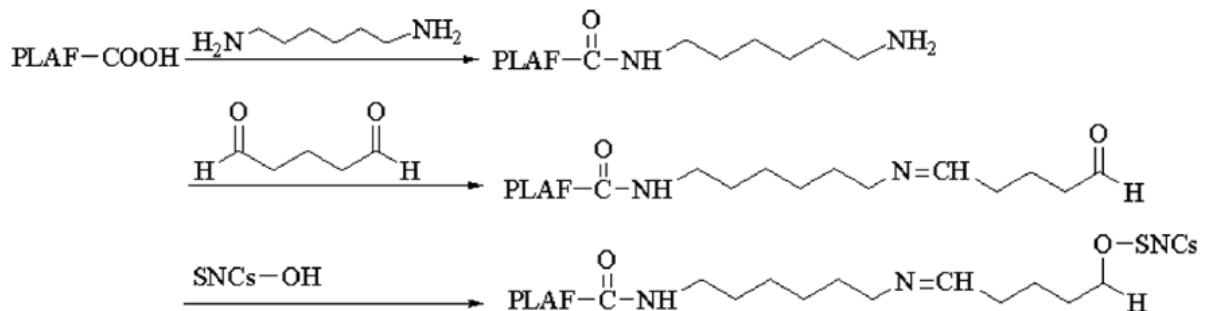


Figure 5: Principle flow chart of grafted SNCs on the surface of PLAF.

of the SNCs and the C-O tensile vibration peak unique to the polysaccharide compound skeleton during grafting modification. From this, it could be proved that the PLAF surface has been successfully grafted with SNCs.

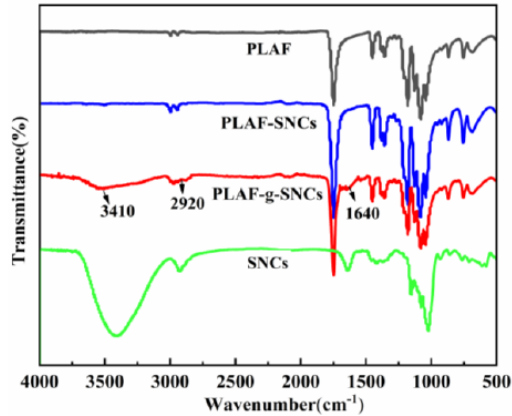


Figure 6: FTIR spectra of PLAF after different treatments.

(3) Grafting Rate of SNCs on the Surface of PLAF

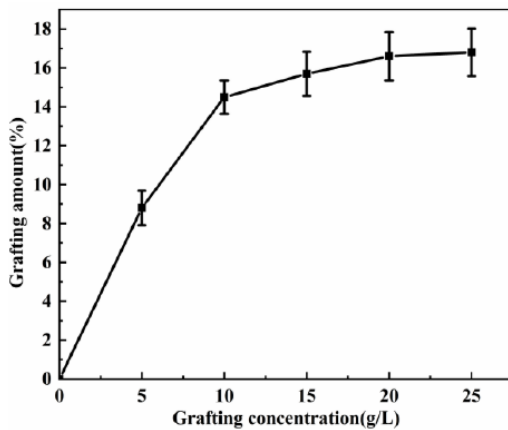


Figure 7: Effect of SNCs content in the treatment solution on the grafting rate.

As shown in Figure 7, the mass of the SNCs grafted on the PLAF surface was determined by weight assay, using the content of the treated liquid SNCs as the variable. It could be seen from Figure 7 that the grafting rate of SNCs gradually increases with the increasing content of starch nanocrystals in the treatment fluid, and the grafting rate does not change much after the content was 15 g/L, but the error of grafting rate was getting bigger and bigger, mainly because with the increase of SNCs in the dispersion, the more obvious, the more unstable the dispersion was, attaching the large particle starch nanocrystals on PLAF surface, affecting the accuracy of its grafting rate. Therefore, when the SNCs in the treated solution were 10 g/L, the starch nanocrystals grafted best with a grafting rate of $14.5\% \pm 0.86\%$.

(4) Thermal Stability Analysis of PLAF

From Figure 8, we showed that a small number of SNCs deposited directly by shock resolved in 150°C , and PLAF was degraded around 263°C , and their thermal stability changed little compared with pure PLAF. However, the content of SNCs on the PLAF surface of chemically grafted SNCs increases, and the introduced SNCs lowers the initial decomposition temperature, but the temperature corresponding to the maximum decomposition rate of PLAF becomes higher, mainly because of the strong interaction between SNCs and chemical bonds on the PLAF surface limits the molecular chain movement of PLAF and increases the decomposition temperature interval of PLAF. Therefore, in the process of fiber and resin composite, the decomposition temperature should be controlled within 150°C .

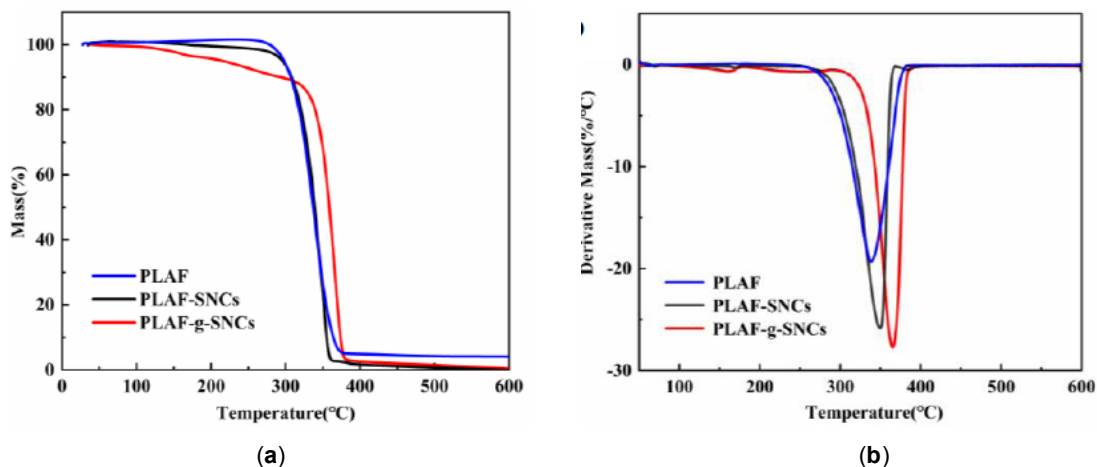


Figure 8: TGA and DTG thermograms of PLAF after different treatments (a) TGA, (b) DTG.

(5) The Surface Morphology Analysis of the PLAF

From Figure 9, the direct observation that PLAF deposited SNCs and only a small amount of SNCs

deposited onto PLAF was not ideal for improving interfacial bonding between PLAF and the starch matrix. However, the PLAF with different

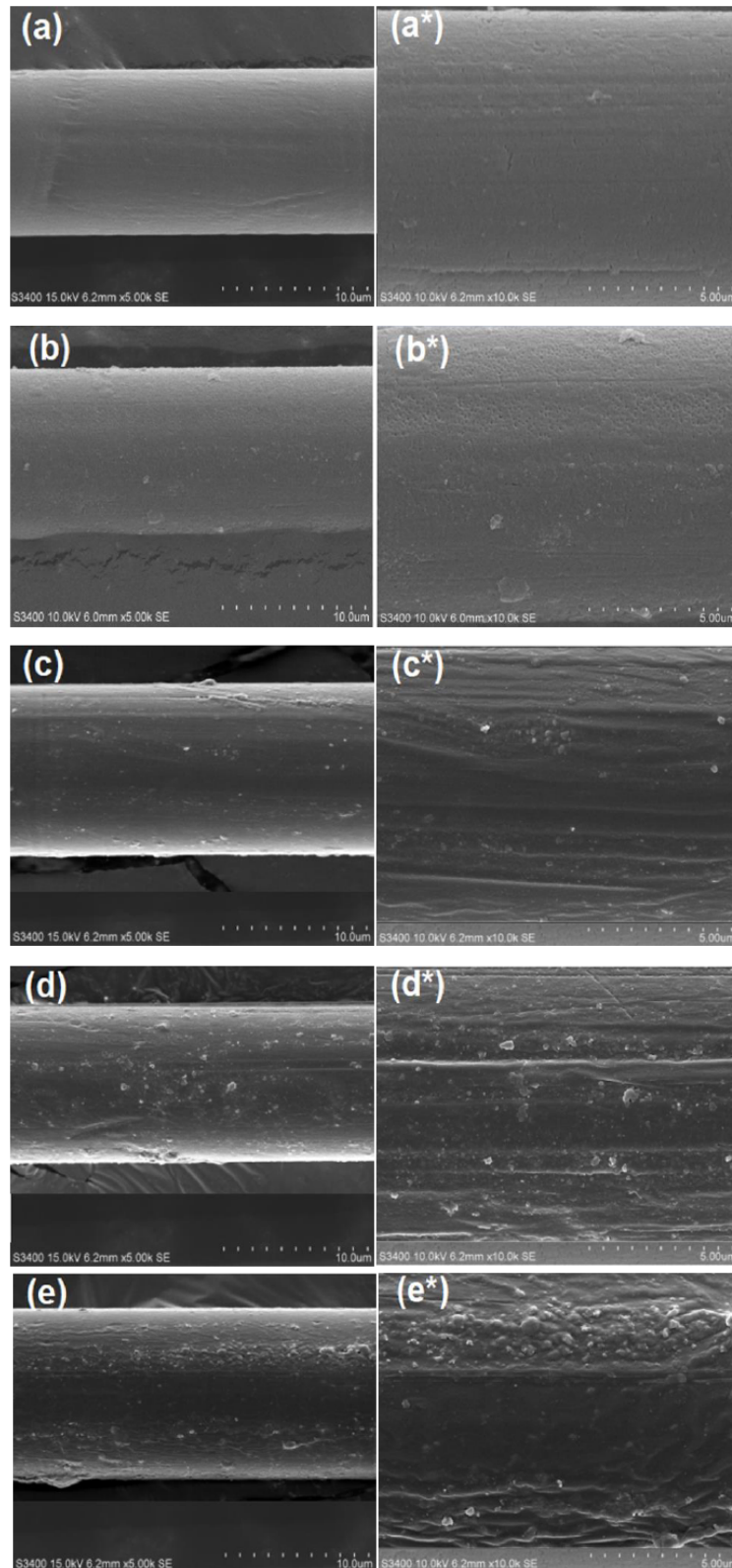


Figure 9: SEM micrographs of PLAF after different treatments.

(a, a*) PLAF, (b, b*) PLAF-SNCs, (c, c*) PLAF-g-SNCs5, (d, d*) PLAF-g-SNCs10, (e, e*) PLAF-g-SNCs15.

concentrations of SNCs became rough, the SNCs particles were evenly distributed, and as the grafting concentration of SNCs increased. However, reunification appeared on the PLAF-g-SNCs15 surface, affecting its interfacial effect [19]. Therefore, the introduction of SNCs at higher concentrations without significant reunion at the PLAF surface showed better interfacial compatibility improvement, corresponding to SNCs grafting rate analysis, thus better selecting PLAF-g-SNCs10 for subsequent experimental exploration.

(6) Analysis of the Moisture Absorption Rate of PLAF

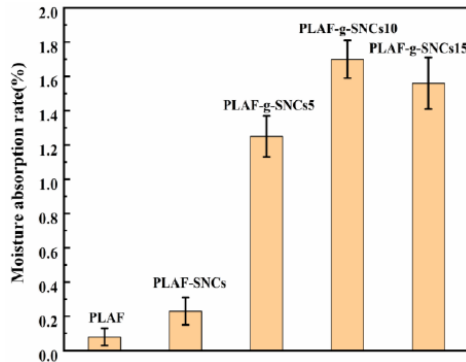


Figure 10: Moisture absorption rate of PLAF after different treatments.

The hydrophilic modification effect of the PLAF surface was analyzed by the size of the water absorption rate. From Figure 10, compared with untreated PLAF, PLAF, while PLAF increased with the content of SNCs, with the overall trend of the first increase and then decreasing. As the nanoparticles of SNCs enter the molecular chain, the internal specific surface area increases with increased moisture absorption rate and increased hydrophilic groups on the surface of SNCs. However, when SNCs were too high, the agglomeration phenomenon was obvious and the distribution of large particles was uneven, resulting in decreased hydrophilic surface area and PLAF.

(7) Analysis of the Tensile Strength of the PLAF

Due to the fiber internal or surface defects and uneven thickness, the tensile strength changes greatly. The Weibull distribution could be used to explore the discretization of fiber strength, and to measure the variability analysis of fiber tensile strength by ranking the fiber's relative strength from its damage probability [20]. As shown in formulas (4) and (5):

$$P(\sigma) = 1 - \exp\left[-\left(\frac{\sigma}{\sigma_0}\right)^m\right], \sigma > 0, \sigma_0 > 0, m > 0 \quad (4)$$

$$\ln\left[\ln\left(\frac{1}{1-P(\sigma)}\right)\right] = m \ln \sigma - m \ln \sigma_0 \quad (5)$$

$P(\sigma)$: Two-parameter Weibull distribution of tensile strength;

m/σ : shape and dimension parameters.

The Weibull distribution inefficiency could be determined by formula for (6):

$$P(\sigma)_i = \frac{i}{n+1} \quad (6)$$

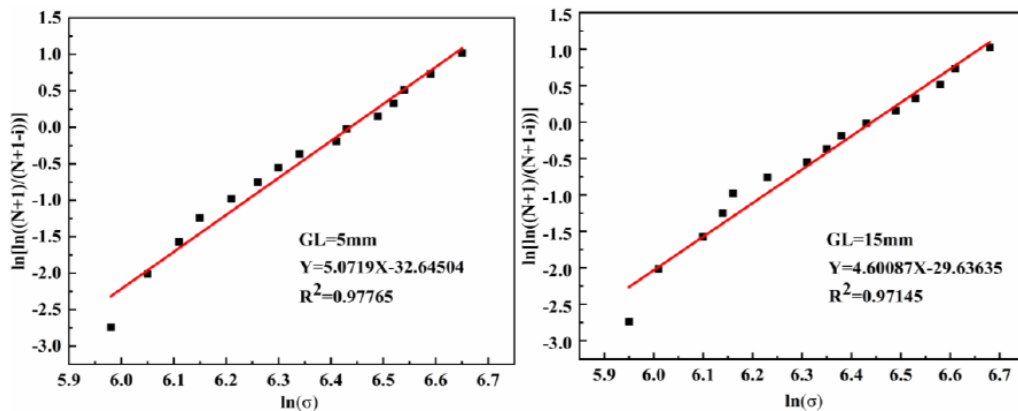
i : sample number order; n : Total number of samples.

The average tensile strength of the PLAF was obtained from formula (7) $\bar{\sigma}$:

$$\bar{\sigma} = \sigma_0 \Gamma\left(1 + \frac{1}{m}\right) \quad (7)$$

1) Effect of the pitch on the tensile strength of the PLAF

In Figure 11, R^2 was between 0.94113 and 0.97765, which showed that the tensile strength of the PLAF showed a good linear distribution relationship. From



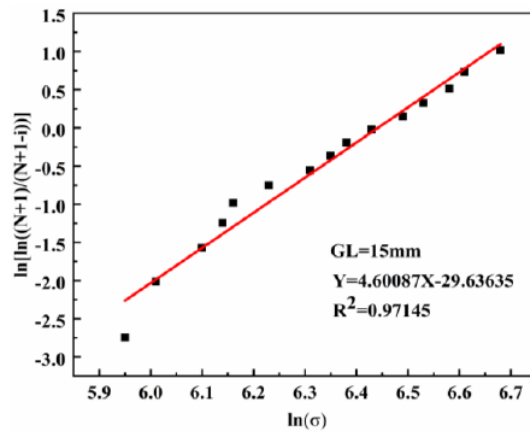


Figure 11: Experimental data and two-parameter Weibull plots for the tensile strength with different standard distances.

Table 1: The Tensile Strength of PLAF with Different Gauge Measurements

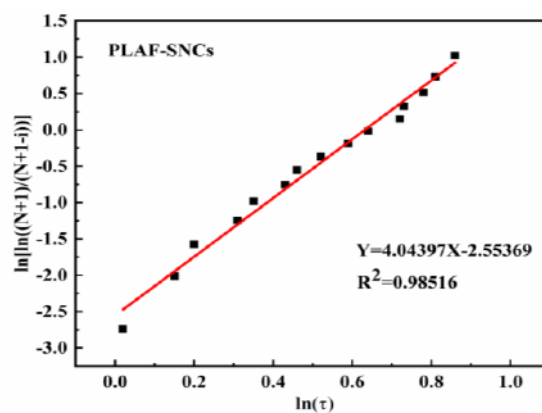
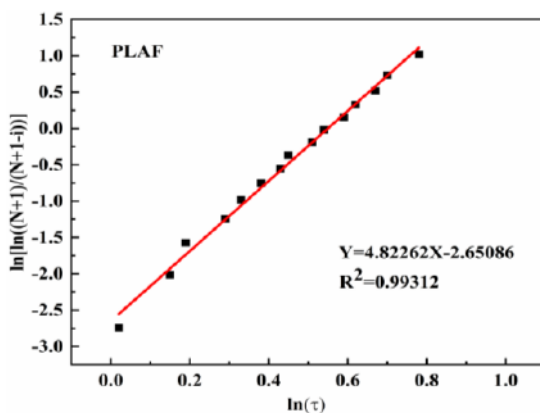
Gauge length(mm)	σ_0 (MPa)	m	$\bar{\sigma}$ (MPa)	R ²
5	626	5.07	575	0.97765
10	678	4.60	620	0.97145
15	628	4.07	569	0.94113

Table 1, as the tensile strength of the fiber decreases m with the stretching process, the tensile strength of the fiber changes greatly with the scale distance. Considering the accuracy of the measurement results and the convenience of the operation instrument, the scale distance value of 10 mm was chosen as the test condition.

2) Tensile strength of PLAF after different treatments

From Figure 12, the R² of the PLAF was between 0.94113-0.98292, with good linear fitting conditions and reasonable experimental data values. It was seen from Table 2 that the tensile strength of untreated PLAF was

around 620 MPa, and the tensile strength of PLAF with directly oscillating deposited SNCs decreases to about 615 MPa, due to a collision with the inner wall of the beaker during the oscillatory deposition. The tensile strength of the PLAF tended to increase with the content of grafted SNCs, but the content of the SNCs increased from 10 g/L to 15 g/L with little change in tensile strength. The amination process damages PLAF, while SNCs as enhancers compensate for the fiber surface damage of the lamination process and have strong chemical bonding to the surface glutaraldehyde, thus improving the tensile strength of PLAF. However, due to the limited grafting amount of SNCs, 10 g/L of SNCs dispersion could provide



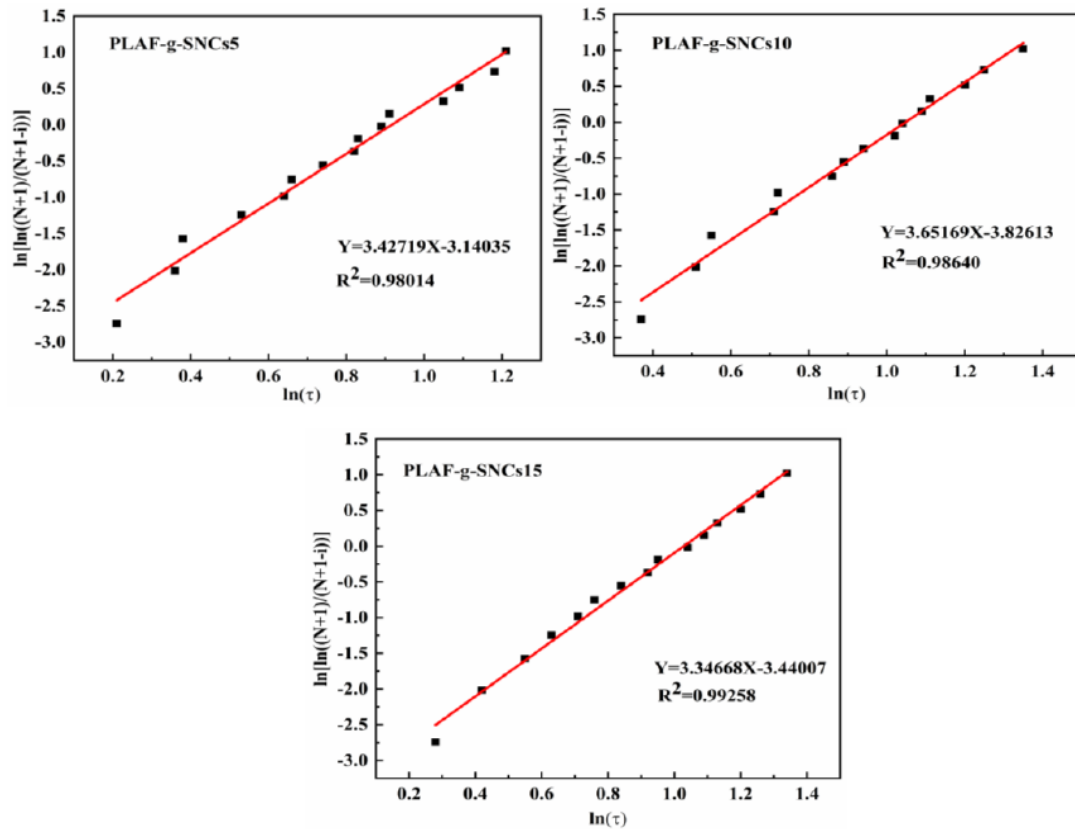


Figure 12: Experimental data and two-parameter Weibull plots for the tensile strength.

Table 2: Tensile Strength of PLAF After Different Treatments

Sample	σ_0 (MPa)	m	$\bar{\sigma}$ (MPa)	R^2
PLAF	678	4.60	620	0.97145
PLAF-SNCs	671	4.88	615	0.98992
PLAF-g-SNCs5	598	5.47	555	0.96069
PLAF-g-SNCs10	639	4.29	582	0.97609
PLAF-g-SNCs15	645	4.40	587	0.98292

enough hydroxyl reaction with glutaraldehyde to form a strong interaction between the two.

(8) Analysis of the Interface Bond Properties of PLAF and Starch

As was known from Figure 13, R^2 values were in the range of 0.98014-0.99312, indicating that the two-parametric Weibull model provides a good linear fit and a reasonable approximation of the experimental data. As could be seen from Table 3, SNCs have a positive effect on improving the interface effect between PLAF

and starch. The interface improvement effect of directly introducing SNCs through physical activity was not obvious, while the IFSS of PLAF was significantly improved by chemical grafting modification, and the optimal IFSS at SNCs concentration content of 10 g/L was 2.57 MPa. Because glutaraldehyde and SNCs form chemical bonds and have stable cross-linking; after the introduction of large hydroxyl and [20] of SNCs, a similar chemical structure to starch was more conducive to improve its interface bond performance [21]. Therefore, the introduction of SNCs on the PLAF

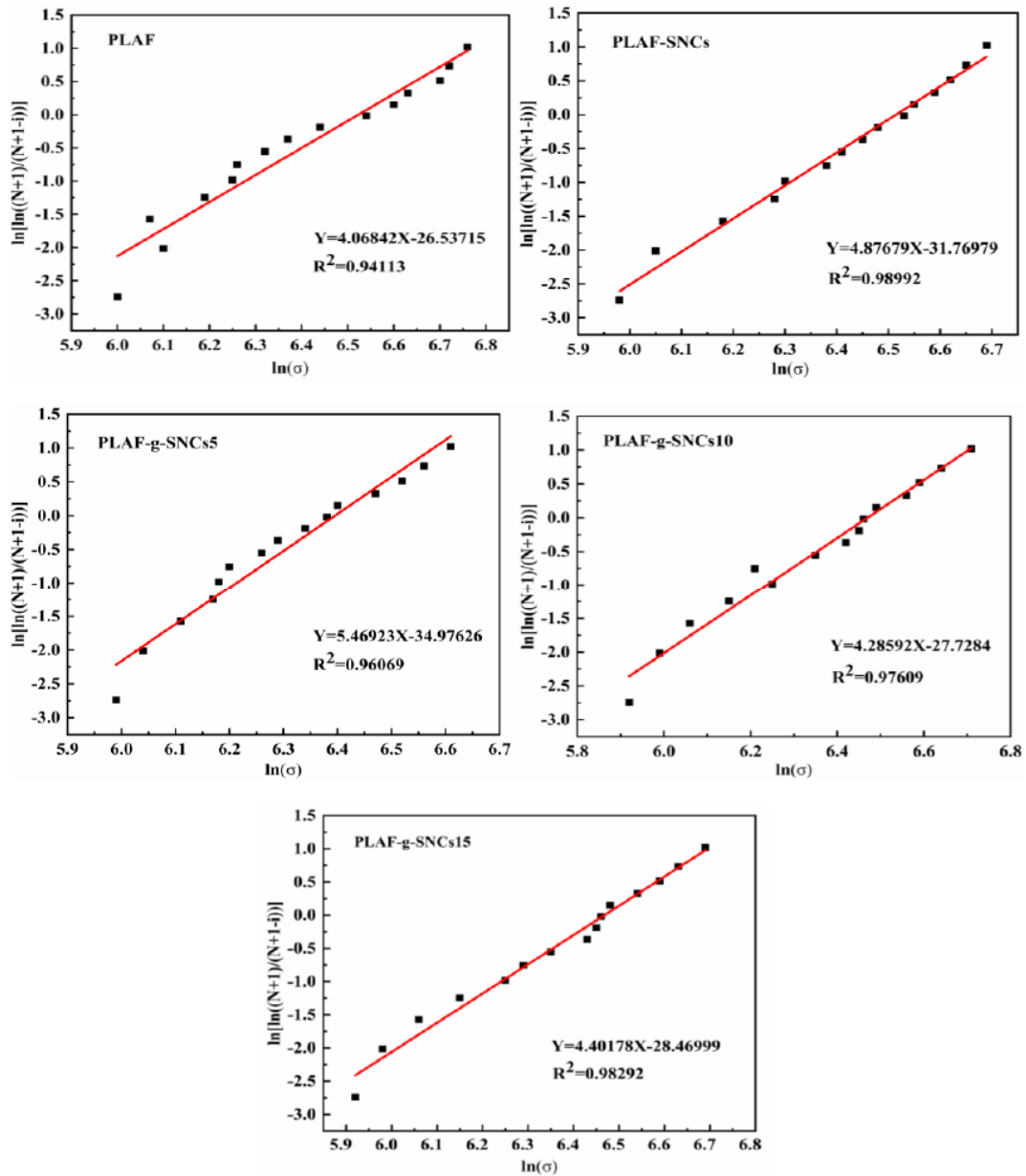


Figure 13: Experimental data and two-parameter Weibull plots for the interfacial shear strength.

Table 3: Interfacial Shear Intensities of PLAFs and Starch after Different Treatments

Sample	τ_0 (MPa)	m	$\bar{\tau}$ (MPa)	R^2
PLAF	1.73	4.82	1.58	0.99312
PLAF-SNCs	1.88	4.04	1.71	0.98516
PLAF-g-SNCs5	2.49	3.43	2.24	0.98014
PLAF-g-SNCs10	2.85	3.65	2.57	0.98640
PLAF-g-SNCs15	2.79	3.35	2.51	0.99258

surface plays an important role in improving the mechanical properties of the composites through chemical binding and physical Locking.

From Figure 14, the interface compatibility between PLAF and starch was poor, and the introduction of SNCs has a positive effect in improving the interface

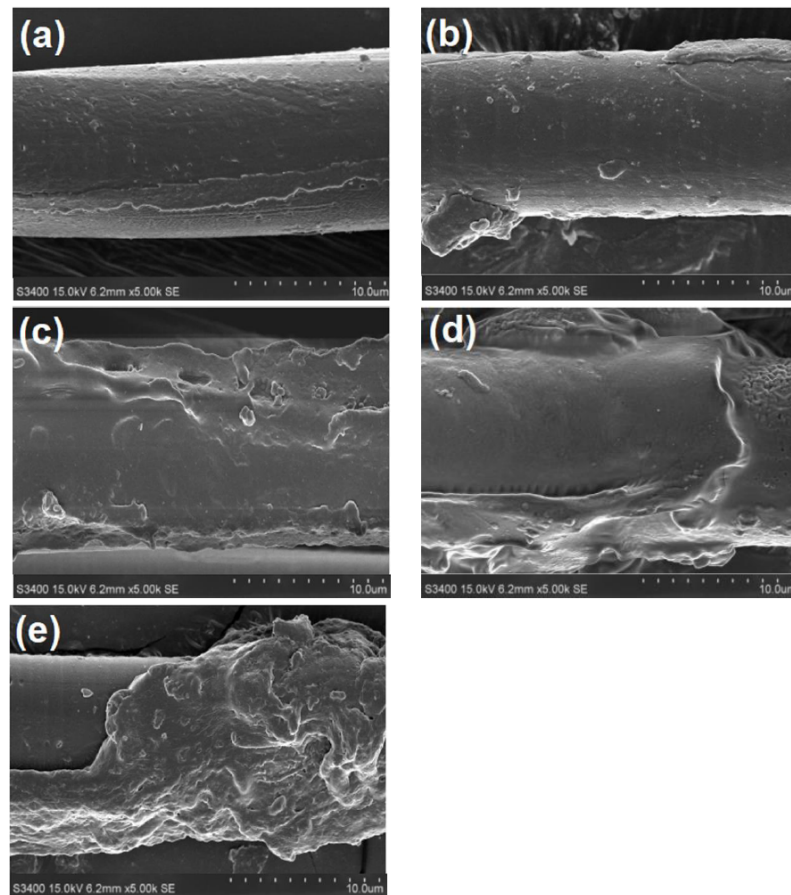


Figure 14: SEM micrographs of PLAF after different treatments. (a) PLAF, (b) PLAF-SNCs, (c) PLAF-g-SNCs5, (d) PLAF-g-SNCs10, (e) PLAF-g-SNCs15.

binding between PLAF and starch. However, PLAF modified by chemical grafted SNCs adhered to a large amount of starch on the surface, indicating that PLAF modified by chemical grafted SNCs formed a strong interface bond with the starch matrix, and the starch underwent cohesion damage under external load. With the increasing concentration of SNCs, the more obvious the interface binding force, the interface shear strength increased by about 63 % relative to the untreated fibers; the starch resin attached to PLAF-g-SNCs 15 surface was fragmented and uneven, which was the relative decrease of IFSS value.

5. CONCLUSION

1. By introducing SNCs to the PLAF surface, chemical grafting SNCs were better than direct oscillatory deposition. When the SNCs content in the treatment solution was 10 g/L, the highest grafting rate was 14.5 ± 0.86 %, and the SNCs were formed through glutaraldehyde, compensating for the fiber surface damage, and PLAF tensile strength could be maintained at around 582 MPa.

2. The modified PLAF interface improved and more hydrophilic. When the SNCs content in the treatment solution was 10 g/L, the PLAF extraction length was 10 mm, and the posterior surface was evenly adhered to a large amount of starch, forming a strong interface bond with the starch matrix, and the highest IFSS value was 2.57 MPa, which increased by about 63 %. Therefore, the introduction of SNCs is important for the interface modification of PLAF and deserves further exploration.

REFERENCE

- [1] Yu X, Chen L, Jin Z, Jiao A (2021) Research progress of starch-based biodegradable materials: a review. *J Mater Sci* 56: 11187-11208. <https://doi.org/10.1007/s10853-021-06063-1>
- [2] Siqueira L, Arias C, Maniglia BC (2020) Starch-based biodegradable plastics: methods of production, challenges, and future perspectives. *Curr Opin Food Sci* 38: 122-130. <https://doi.org/10.1016/j.cofs.2020.10.020>
- [3] Heidarian P, Behzad T, Sadeghi M (2017) Investigation of cross-linked PVA/starch biocomposites reinforced by cellulose nanofibrils isolated from aspen wood sawdust. *Cellulose* 24: 3323-3339. <https://doi.org/10.1007/s10570-017-1336-4>

- [4] Zhang YC, Rempel C, Liu Q (2014) Thermoplastic starch processing and characteristics-a review. *Food Sci Nutr* 54: 1353-1370.
<https://doi.org/1080/10408398.2011.636156>
- [5] Ashogbon AO, Akintayo ET (2014) Recent trend in the physical and chemical modification of starches from different botanical sources: a review. *Starch-Starke* 66: 41-57.
<https://doi.org/10.1002/star.201300106>
- [6] Gao J, Luo ZG, Luo FX (2012) Ionic liquids as solvents for dissolution of corn starch and homogeneous synthesis of fatty-acid starch esters without catalysts. *Carbohydr Polym* 89: 1215-1221.
<https://doi.org/10.1016/j.carbpol.2012.03.096>
- [7] Savadekar NR, Mhaske ST (2012) Synthesis of nano cellulose fibers and effect on thermoplastics starch based films. *Carbohydr Polym* 89: 146-151.
<https://doi.org/10.1016/j.carbpol.2012.02.063>
- [8] Chang Y, Sun T, Fan C, Zhou X (2018) The effect of surface modification on the properties of sisal fiber and improvement of interfacial adhesion in sisal/starch composites induced by starch nanocrystals. *Compos Interfaces* 25: 1-14.
<https://doi.org/10.1080/09276440.2018.1450586>
- [9] Jiang L, Liu B, Zhang JW (2009) Novel high-strength thermoplastic starch reinforced by in situ poly(lactic acid) fibrillation. *Macromol Mater Eng* 294: 301-305.
<https://doi.org/10.1002/mame.200900018>
- [10] Weng F, Wang M, Ernest K, Ma N, Wu Z, Wu Q (2018) Effects of pba-based polyurethane prepolymer as compatibilizer on the properties of polylactic acid-starch composites. *Starch-Starke* 71: 3-4.
<https://doi.org/10.1002/star.201800205>
- [11] Sreekumar PA, Thomas SP, Saiter JM, Joseph K, Unnikrishnan G, Thomas S (2009) Effect of fiber surface modification on the mechanical and water absorption characteristics of sisal/polyester composites fabricated by resin transfer molding. *Compos Pt A-Appl Sci Manuf* 40: 1777-1784.
<https://doi.org/10.1016/j.compositesa.2009.08.013>
- [12] Angellier H, Choïnard L, Molina-Boisseau S (2009) Optimization of the Preparation of Aqueous Suspensions of Waxy Maize Starch Nanocrystals Using a Response Surface Methodology. *Biomacromolecules* 5: 1545-1551.
<https://doi.org/10.1049/el:20071208>
- [13] Chen Y, Zhou X, Yin X, Lin Q, Zhu M (2013). A novel route to modify the interface of glass fiber-reinforced epoxy resin composite via bacterial cellulose. *Int J Polym Mater Polym Biomat* 63: 221-227.
<https://doi.org/10.1080/00914037.2013.830250>
- [14] Liu C, Li K, Li X, Zhang M, Li J (2021). Formation and structural evolution of starch nanocrystals from waxy maize starch and waxy potato starch. *Int J Biol Macromol* 180: 625-632.
<https://doi.org/10.1016/j.ijbiomac.2021.03.115>
- [15] Chang Y, Sun TS, Fan C, Zhou, XD (2018) The effect of surface modification on the properties of sisal fiber and improvement of interfacial adhesion in sisal/starch composites induced by starch nanocrystals. *Compos Interfaces* 25: 1-14.
<https://doi.org/10.1080/09276440.2018.1450586>
- [16] Arbelaz A, Cantero G, B. Fernández, Mondragon I, Kenny JM (2010) Flax fiber surface modifications: effects on fiber physico mechanical and flax/polypropylene interface properties. *Polymer Composites*, 26: 324-332.
<https://doi.org/10.1002/pc.20097>
- [17] Li C, Sun PD, Yang C (2018) Emulsion stabilized by starch nanocrystals. *Starch-Starke*, 64: 497-502.
<https://doi.org/10.1002/star.201100178>
- [18] ihem, Bel, Haaj, Albert, Magnin, Christian, Pétrier, Sami, Boufi (2013) Tarch nanoparticles formation via high power ultrasonication. *Carbohydr Polym* 92: 1625-1632.
<https://doi.org/10.1016/j.carbpol.2012.11.022>
- [19] Wu G, Ma L, Li L, Wang Y, Fei X, Zhong Z (2016) Interface enhancement of carbon fiber reinforced methylphenylsilicone resin composites modified with silanized carbon nanotubes. *Mater Des* 89: 1343-1349.
<https://doi.org/10.1016/j.matdes.2015.10.016>
- [20] Flavio de Andrade Silva, Nikhilesh Chawla, Romildo Dias de Toledo Filho (2009) Tensile behavior of high performance natural (sisal) fibers. *Compos Sci Technol* 68: 3438-3443.
<https://doi.org/10.1016/j.compscitech.2008.10.001>
- [21] Chen Y, Liu C, Chang PR, Cao X, Anderson DP (2009) Bionanocomposites based on pea starch and cellulose nanowhiskers hydrolyzed from pea hull fibre: effect of hydrolysis time. *Carbohydr Polym* 76: 607-615.
<https://doi.org/10.1016/j.carbpol.2008.11.030>

Received on 24-10-2022

Accepted on 17-11-2022

Published on 24-11-2022

DOI: <https://doi.org/10.12974/2311-8717.2022.10.02>

© 2022 Sun et al.

This is an open access article licensed under the terms of the Creative Commons Attribution Non-Commercial License (<http://creativecommons.org/licenses/by-nc/3.0/>) which permits unrestricted, non-commercial use, distribution and reproduction in any medium, provided the work is properly cited.